Accepted on February 20, 2018 for publication in J. Climate

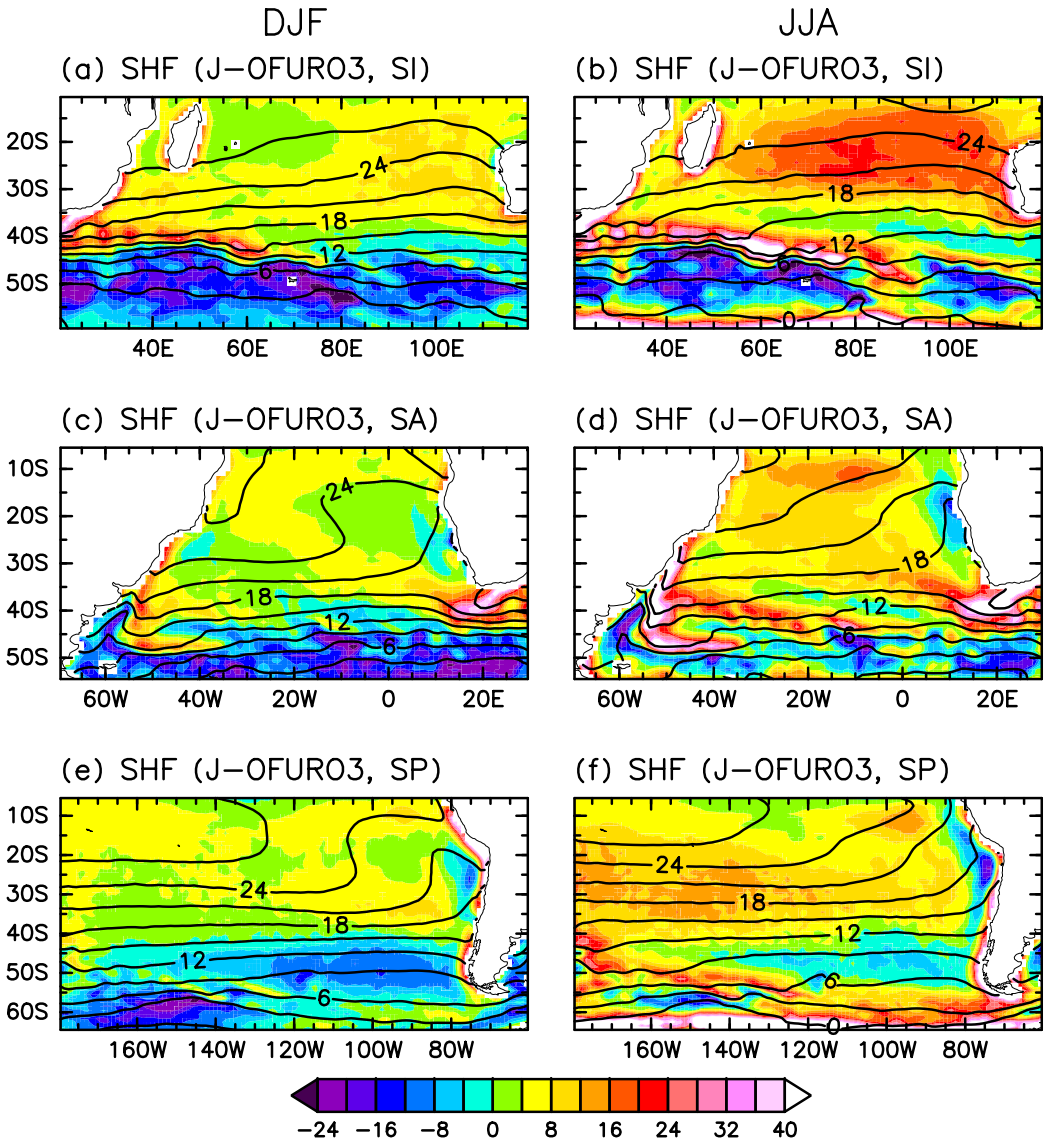

Fig. S1: Climatological distributions for austral summer (DJF) of maritime surface sensible heat flux (SHF; color shaded for every 4 W m^{-2}) over (a) the South Indian Ocean, (c) the South Atlantic, and (e) the South Pacific based on J-OFURO3. Superimposed with contours is SST (every 3 °C) in ERA-Interim. (b), (d) and (f) Same as in (a), (c) and (e), respectively, but for austral winter (JJA). (a-f) correspond to Figs. 2i, 2j, 11g, 11h, 12g and 12h, respectively.

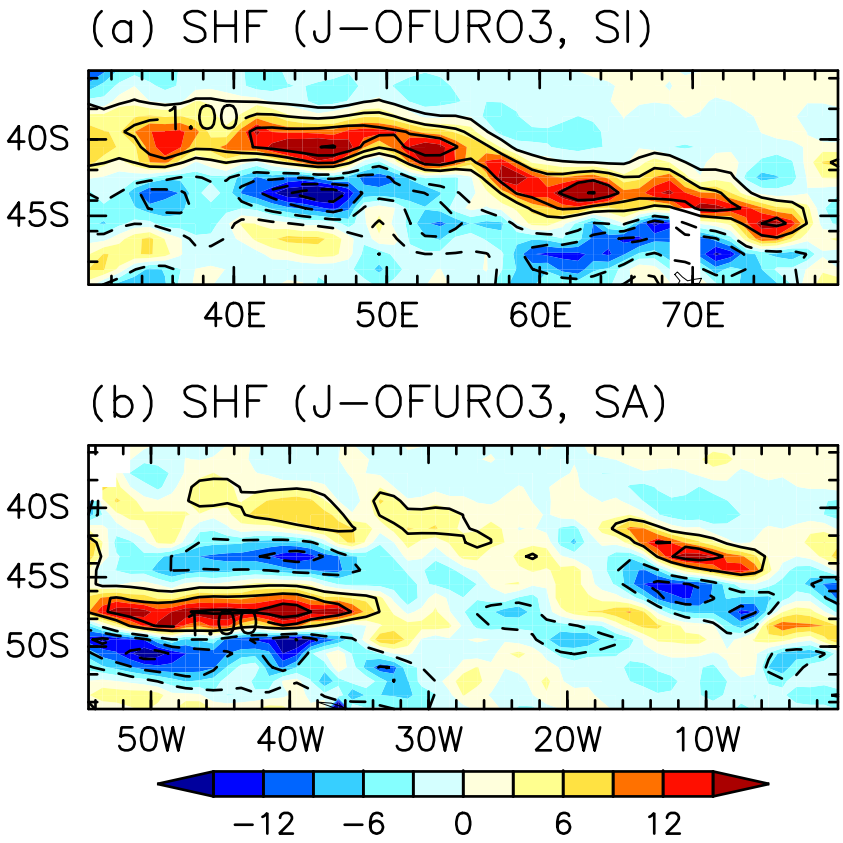

Fig. S2: Meridionally high-pass-filtered fields for austral summer (DJF) of SHF (color shaded for every 3 W m^{-2}) based on J-OFURO3 over (a) the South Indian Ocean and (b) the South Atlantic. Superimposed with the contours is meridionally high-pass-filtered SST in ERA-Interim (every 0.5 °C; solid and dashed lines for positive and negative values, respectively) for DJF. Local departures of each variable from its meridional nine-point running-mean values are regarded as the meridionally high-pass-filtered components. (a-b) correspond to Figs. 3d and 13c, respectively.

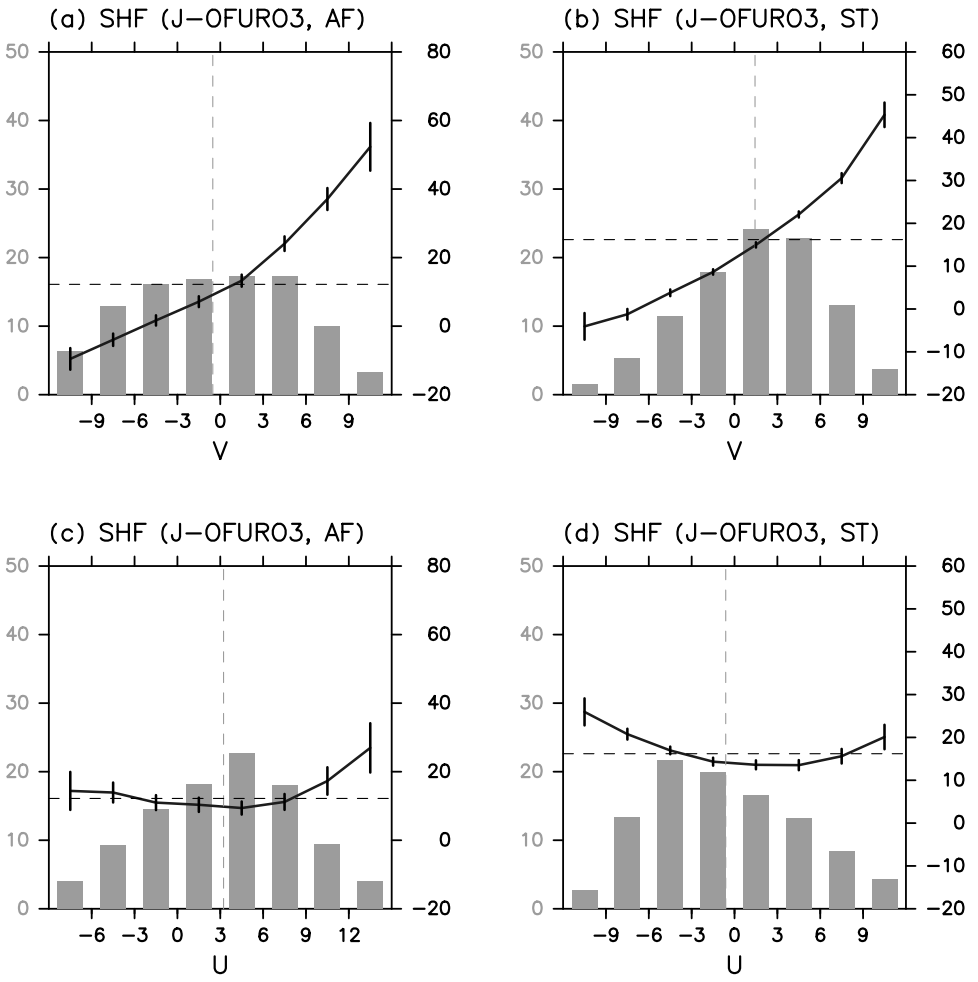

Fig. S3: (a) Dependence of daily SHF (W m^{-2}; right ordinate) in J-OFURO3 on surface meridional wind velocity in ERA-Interim in DJF. Grey bars are daily frequency (%; left ordinate) of surface meridional wind (m s^{-1}) at individual grid points within the domain on the equatorward flank of the Agulhas SST front [40.5°E-54.5°E, 37.5°S-41.5°S, AF]. Tick marks along the abscissa indicate bin boundaries. Leftmost and rightmost bars include all the samples of the strongest northerlies and southerlies, respectively. Black solid line indicates climatological-mean values of SHF (right ordinate) for individual bins with the 90% confidence intervals, while the climatological-mean SHF averaged over all the samples is represented by the black dashed horizontal line. The grey dashed vertical line indicates the climatological-mean meridional wind. (b) Same as in (a), but for the equatorward flank of the subtropical SST front [60.5°E-109.5°E, 27.5°S-29.5°S, ST] in JJA. (c-d) Same as in (a-b), respectively, but for the dependence of SHF on surface zonal wind velocity. (a-d) correspond to Figs. 4a, 8a, 4d and 8d, respectively.

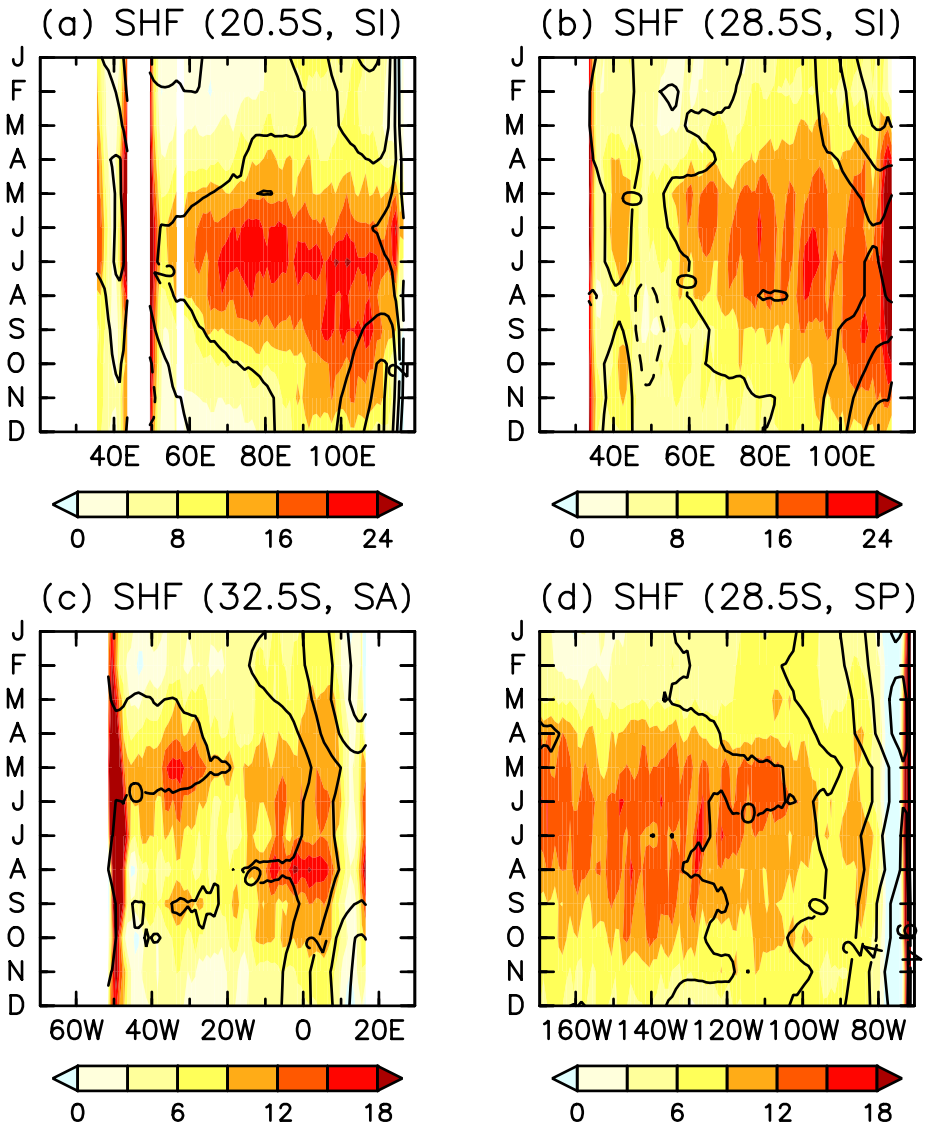

Fig. S4: Climatological-mean seasonal cycle of the longitudinal distribution of SHF (W m^{-2}; coloring convention is indicated at the bottom of each panel) in J-OFURO3 across the subtropical basin of (a) the South Indian Ocean at 20.5°S, (b) the South Indian Ocean at 28.5°S, (c) the South Atlantic at 32.5°S and (d) the South Pacific at 28.5°S. The corresponding seasonal cycle of the meridional component of surface winds (every 2 m s^{-1}; positive values for the southerlies) in ERA-Interim are superimposed with contours. (a-d) correspond to Figs. 6e, 7e, 14e and 14j, respectively.

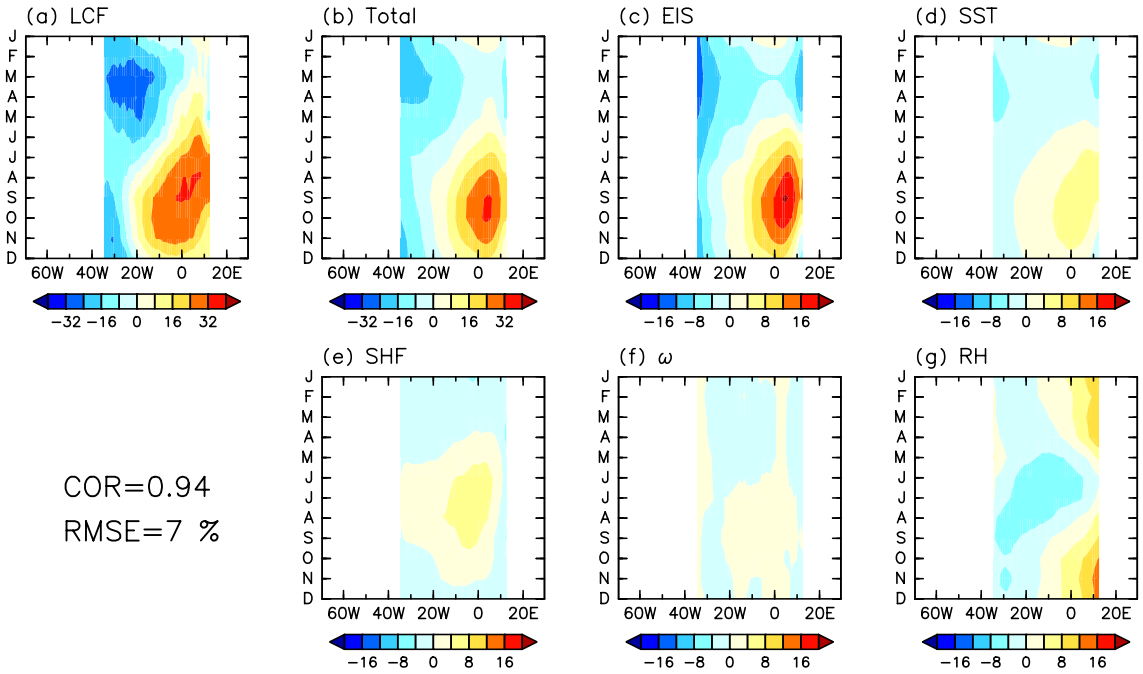

Fig. S5: (a) Climatological-mean seasonal cycle of the longitudinal distribution of low-cloud fraction (LCF, %) across the subtropical basin of the South Atlantic at 10.5°S. The annual-mean LCF within the domain has been removed. (b) Same as in (a), but for the corresponding LCF (%) predicted by the multiple linear regression model described in Appendix B. The correlation and root mean square error (RMSE) between (a) and (b) are shown below the panel (a). (c-g) Same as in (b) but for the contributions from EIS, SST, SHF, 700-hPa ω, and 700-hPa RH, respectively, to (b). For each of the panels coloring convention is indicated at the bottom.

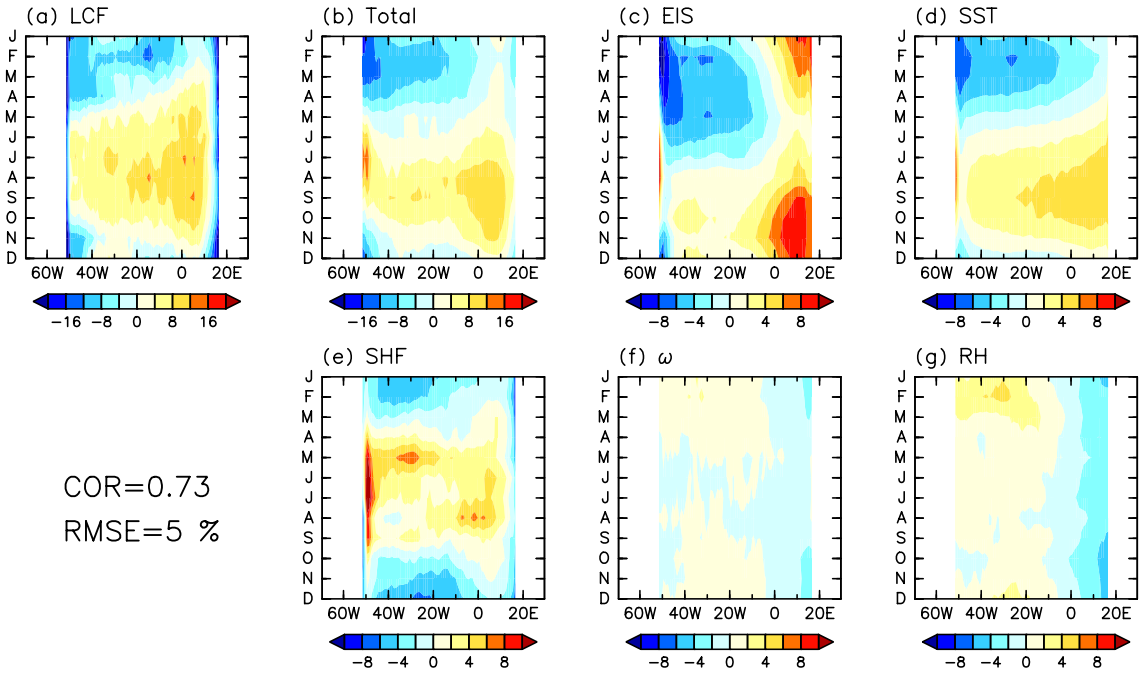

Fig. S6: Same as in Fig. S5, but for the South Atlantic at 32.5°S.

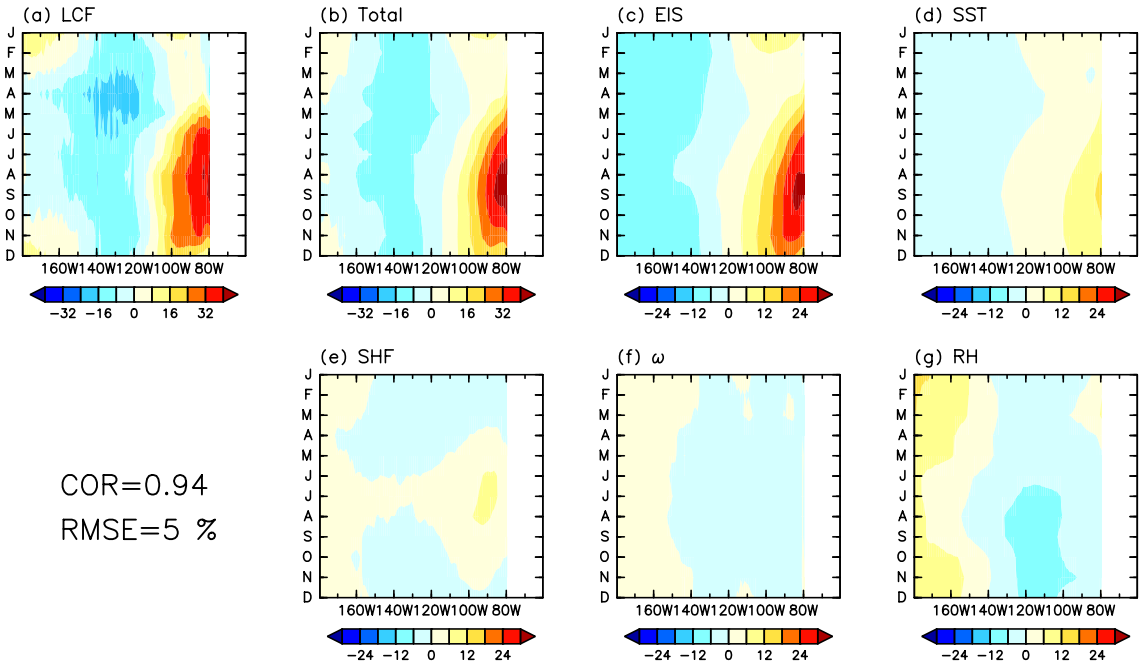

Fig. S7: Same as in Fig. S5, but for the South Pacific at 10.5°S.

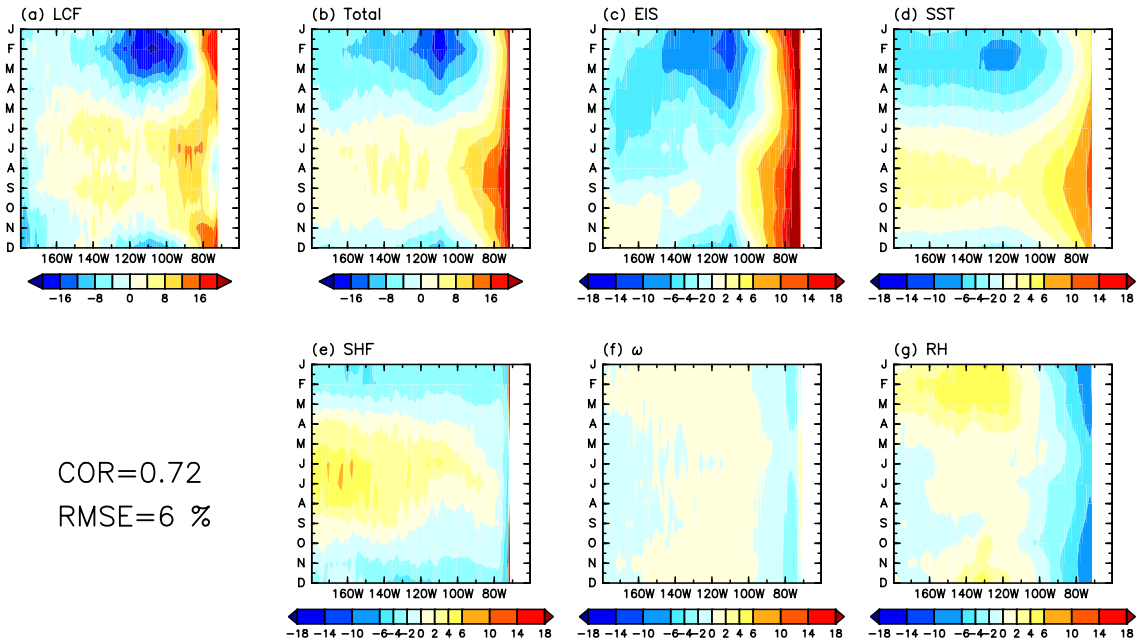

Fig. S8: Same as in Fig. S5, but for the South Pacific at 28.5°S.